 doi:10.20944/preprints202205.0349.v1

Screening and identification of novel small molecule inhibitors against *Mycobacterium tuberculosis* Dihydrodipicolinate synthase enzyme using *in silico* and *in vitro* methods

Anasuya Bhargav[#1,2], Pratibha Chaurasia[#1,2], Nikita V. Ivanisenko[3], Vladimir A. Ivanisenko[3], Bhupesh Taneja[1,2], Srinivasan Ramachandran[1,2*]

#equal contributors

* corresponding author

[1]Council of Scientific and Industrial Research – Institute of Genomics and Integrative Biology (CSIR-IGIB), Mathura Road, New Delhi, 110025 India

[2]Academy of Scientific and Innovative Research (AcSIR), Ghaziabad- 201002, India

[3]Institute of Cytology and Genetics SB RAS, Novosibirsk, Russia

Abstract

Emergence of multi drug resistant (MDR) and extensively drug resistant (XDR) *Mycobacterium tuberculosis* poses a serious threat to TB control as the available treatment options are less effective in these cases. Therefore, new strategies are required for identification of new drugs and drug targets. The *M. tuberculosis* dihydrodipicolinate synthase is a putative drug target with no potent inhibitor. Here in this study, we have used a comprehensive computational approach to identify small molecule inhibitors and validated them *in vitro*. As similar structures tend to have similar functions, therefore 3 approaches, namely, (a) known inhibitor-based approach, (b) substrate analogues, (c) product analogues were used for compound screening from various chemical libraries. The fourth approach we have taken is fragment library screening.

 doi:10.20944/preprints202205.0349.v1

In vitro studies revealed that β-hydroxypyruvic acid tartronic acid are inhibitors of Mtb-rDapA with maximum inhibition 48% and 51% at 500µM concentrations respectively. We have also observed that β-hydroxypyruvic acid is a time dependent inhibitor of Mtb-rDapA. Further, thermal shift assays showed that β-hydroxypyruvic acid interacts with Mtb-rDapA and the thermal stability of Mtb-rDapA shifted by 3˚C. Among the product analogues of Mtb-DapA, dipicolinic acid showed to bind to Mtb-rDapB shifting thermal stability of Mtb-rDapB by 0.5˚C in binding. Additionally, we have designed a new approach by combining substrate and product analogues to achieve better inhibitions. *In vitro* assays validated that this combination approach increased maximum inhibition up to 100%. We envision that these compounds would serve as potent leads for tuberculosis drug discovery.

Keywords: Docking, lead discovery, molecular dynamic simulation, tuberculosis, coupled assay

1. Introduction

Tuberculosis (TB) is a communicable disease and is one of the top 10 causes of deaths worldwide. The disease is caused by the bacillus *Mycobacterium tuberculosis* (Mtb). According to World Health Organization's 2020 Global Tuberculosis Report, about 10 million people got TB infections in 2019, out of which 1.4 million died [1]. Emergence of multi drug resistant (MDR) and extensively drug resistant (XDR) *M. tuberculosis* poses a serious threat to TB control as the available treatment options are less effective in these cases. Therefore, new strategies are required for identification of new drugs and drug targets.

The mycobacterial cell wall has a particularly distinguishing feature consisting of mycolyl-arabinogalactan- peptidoglycan (mAGP) complex [2]. The peptidoglycan chains are interconnected by a tetrapeptide side chain consisting of L-alanine, D-glutamic acid, meso-diaminopimelic acid (mDAP) and D-alanine. mDAP is synthesized by diaminopimelate (DAP)

 doi:10.20944/preprints202205.0349.v1

pathway, which is also the synthetic pathway for the essential amino acid lysine [3]–[5] in *M. tuberculosis* (Mtb). This pathway is conserved[6] and essential because absence of DAP results in cell lysis and death [7]. Further, this pathway is absent in human and therefore the DAP pathway is a suitable drug target.

In the first step of DAP pathway, aspartokinase catalyzes the phosphorylation of L-aspartate to L-β -aspartyl-4-phosphate. The second step is the conversion to L-aspartate-beta-semialdehyde (ASA) by aspartate semialdehyde dehydrogenase. This is followed by a Schiff base formation with pyruvate and condensation of ASA to form (4S)-4-hydroxy-2,3,4,5-tetrahydro-(2S)-dipicolinate (HTPA) catalyzed by dihydrodipicolinate synthase (DapA) . Next, HTPA is reduced to 2,3,4,5-tetrahydrodipicolinic acid (THDP) catalyzed by dihydrodipicolinate reductase (DapB) using NADPH as an electron donor. THDP then undergoes a series of biochemical transformations to yield meso-diaminopimelate (m-DAP) and lysine. In this study, we have focussed on Mtb-DapA and Mtb-DapB enzymes as the enzyme Mtb-DapA catalyses the 1st committed step of the pathway. The crystal structures of both these enzymes are available.

The three-dimensional structure of Mtb-DapA was determined earlier and refined at 2.28 Å (PDB ID 1XXX) [8]. The crystal structure reveals a tetrameric state of the enzyme with 4 identical subunits. Each tetramer is a dimer of dimers, where two monomers are bound to each other to form a tight dimer. The functionally important residue of the active site of the enzyme is Lys171, underlying key catalytic role in the Schiff base formation. The Mtb-DapB crystal structure was resolved in complex with NADPH and dipicolinic acid (PDB ID 1C3V). Mtb-DapB is a tetramer of identical subunits, with each subunit composed of two domains connected by two flexible hinge regions [9].

 doi:10.20944/preprints202205.0349.v1

Several attempts have been made in search for potent inhibitors against DAP enzymes [10]–[13], but but a potent inhibitor still to be found for a better inhibitor remains. Several structural analogues of natural substrate pyruvate were studied by Karsten et al. against *E. coli* DapA [14]. Among them, α-ketobutyrate (Ki= 0.83mM) and α-ketovalerate (Ki= 0.7mM) are carboxylic acids having keto group at alpha position similar to pyruvate, only with higher carbon chain lengths. Glyoxalate, a 2-carbon carboxylic acid having aldehyde group had the lowest Ki of 0.016mM against E. coli DapA. Further, they have also reported 3-fluoropyruvate, fluorinated analogue of pyruvate, with Ki 0.22mM [14]. Along the same line, alpha-ketopimelic acid (αKPA) was reported as a potent Mtb-rDapA inhibitor with maximum inhibition of 88% and IC50 21µM [11]. Further, 8 conformationally constrained diketopimelic acid analogues were tested against *E. coli* DapA, with maximum inhibition observed at 49% at 5mM concentration [15]. The reaction intermediate mimics of *E. coli* DapA namely, dipicolinic acid and isopthalic acids were studied as competitive inhibitors [16]. Piperidine and pyridine-2,6-dicarboxylate analogues, including N-oxide of dipicolinic acid and di-imidate of dimethyl pyridine-2,6-dicarboxylate were studied previously. These compounds were reported to have IC50 value of 0.2 mM against the *E. coli* DapA [10], [17]. Turner et al. designed 2 irreversible inhibitors diethyl (E)-4-oxo-2-heptenedioate and diethyl (E, E)-4-oxo-2,5-heptadienedioate mimicking reaction intermediate 4-hydroxytetrahydrodipicolinate. These compounds showed only 50% inhibition at concentration range 0.5–50mM [18].

In this work we have used a comprehensive computational approach to identify small molecule inhibitors and validated them *in vitro*. As similar structures tend to have similar functions [19], therefore 3 approaches, namely, (a) known inhibitor-based approach, (b) substrate analogues, (c) product analogues were used for compound screening from various chemical libraries. The fourth approach we have taken is fragment library screening. The known inhibitor-based approach was based on our previous report of αKPA being Mtb-DapA inhibitor [11]. Further,

 doi:10.20944/preprints202205.0349.v1

from the same study, several rules had been deduced for designing Mtb-DapA inhibitors, such as optimum carbon chain length, presence of keto or hydroxyl group at alpha position. This study is a continuation to the previous report and we have added knowledge onto the rules for chemical inhibitor screening.

2.Materials and Methods:

2.1 Ligand dataset:

Ligands were shortlisted using 4 different approaches:

a) *Known inhibitor-based screening*: For structure similarity search, αKPA was used as start compound [11] and screening of the compounds with keto group was carried out from chemical libraries. Ligands were retrieved from PubChem [20] (https://pubchem.ncbi.nlm.nih.gov/) and ZINC [21] (https://zinc.docking.org/) databases as ready-to-dock compounds (**Figure 1**). As similar structured tend to have similar functions, therefore initially compounds with ≥90% structure similarity was screened from PubChem and ZINC databases. Following to that, extended PubChem search was carried out to retrieve all compounds with ≥70% structure similarity with αKPA.

b) *Substrate analogue study:* Pyruvate is one of the substrates of Mtb-DapA enzyme. Compounds designed by substituting pyruvate with functional groups like methyl, hydroxyl, carboxyl are shown in **Figure 2**. A few compounds were also designed by substituting fluorine (F) at different positions. Due to the small size and high electronegativity of fluorine, these compounds are expected to be highly polar. Substrate analogues were selected from Sigma-Aldrich Commercial compound library [22] (**Figure 3a**).

Preprints (www.preprints.org) | NOT PEER-REVIEWED | Posted: 25 May 2022 doi:10.20944/preprints202205.0349.v1

c) *Product analogue study:* Product analogues of Mtb-DapA enzyme were shortlisted from Sigma-Aldrich chemical library [22]. In silico screening of product analogues were performed against Mtb-DapB protein (**Figure 3b**).

d) *Fragment library screening:* Fragments are small molecular weight compounds with the ability to bind to different parts of target and cover a large chemical space. Enamine golden library (shared by José A. Marquez group at European Molecular Biology Laboratory (EMBL) Grenoble) [23] with 1204 active fragments was screened against Mtb-DapA protein (**Figure 3c**). These were obtained in SMILES format, which were converted into 3D structure files using the open-source cheminformatics tool RDKit [24]. The ligand data file was read into a pandas DataFrame followed by salt removal, hydrogen addition and converting the SMILES into 3D SDF files.

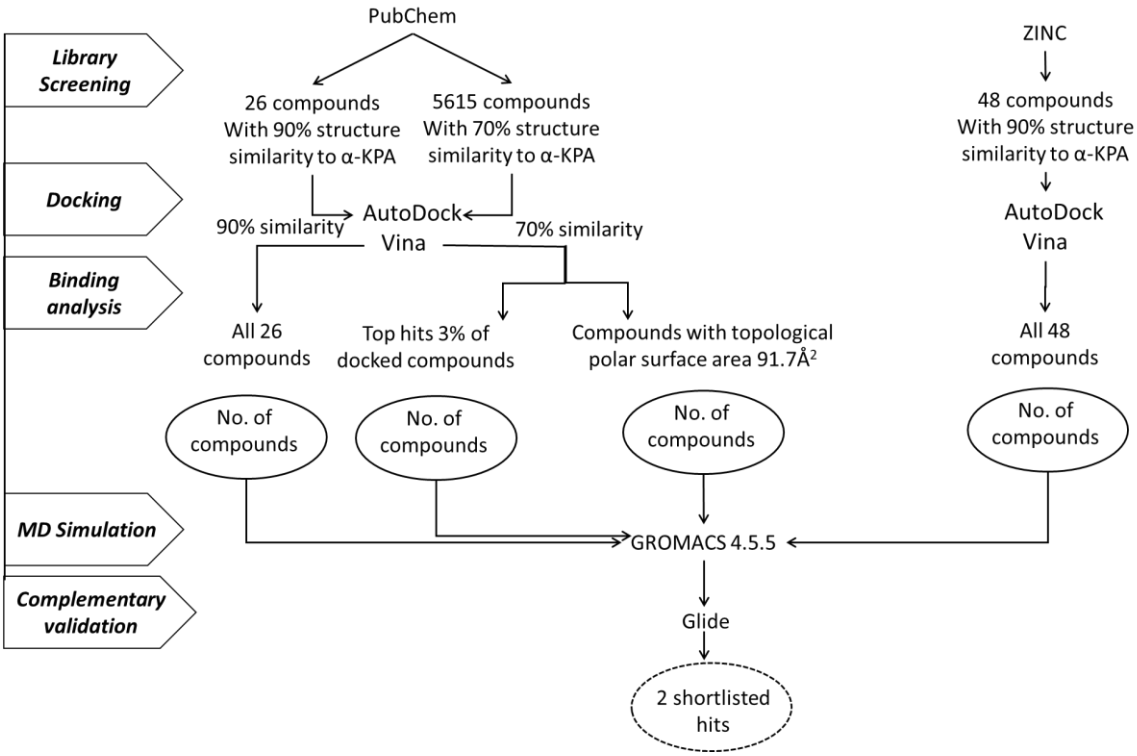

Figure 1: Step by step methodology for known inhibitor-based screening

Preprints (www.preprints.org) | NOT PEER-REVIEWED | Posted: 25 May 2022 doi:10.20944/preprints202205.0349.v1

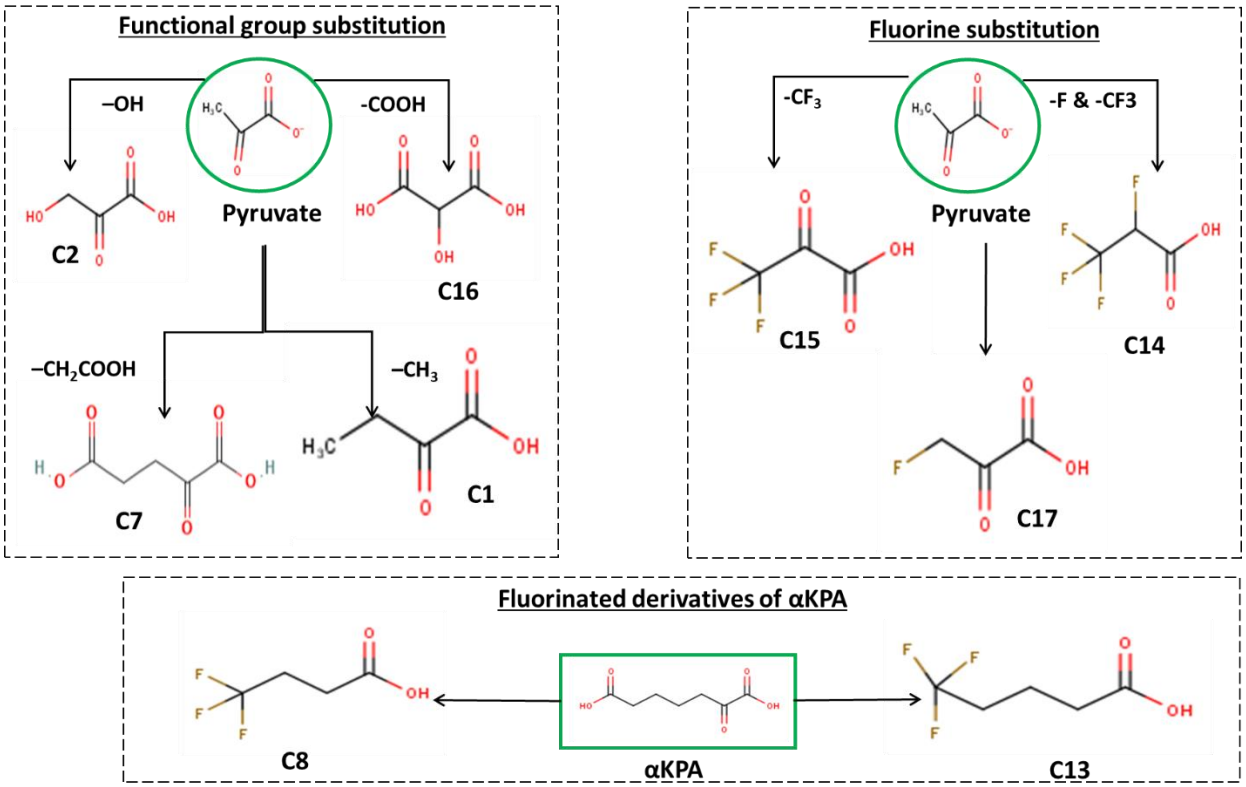

Figure 2: Design of substrate analogues

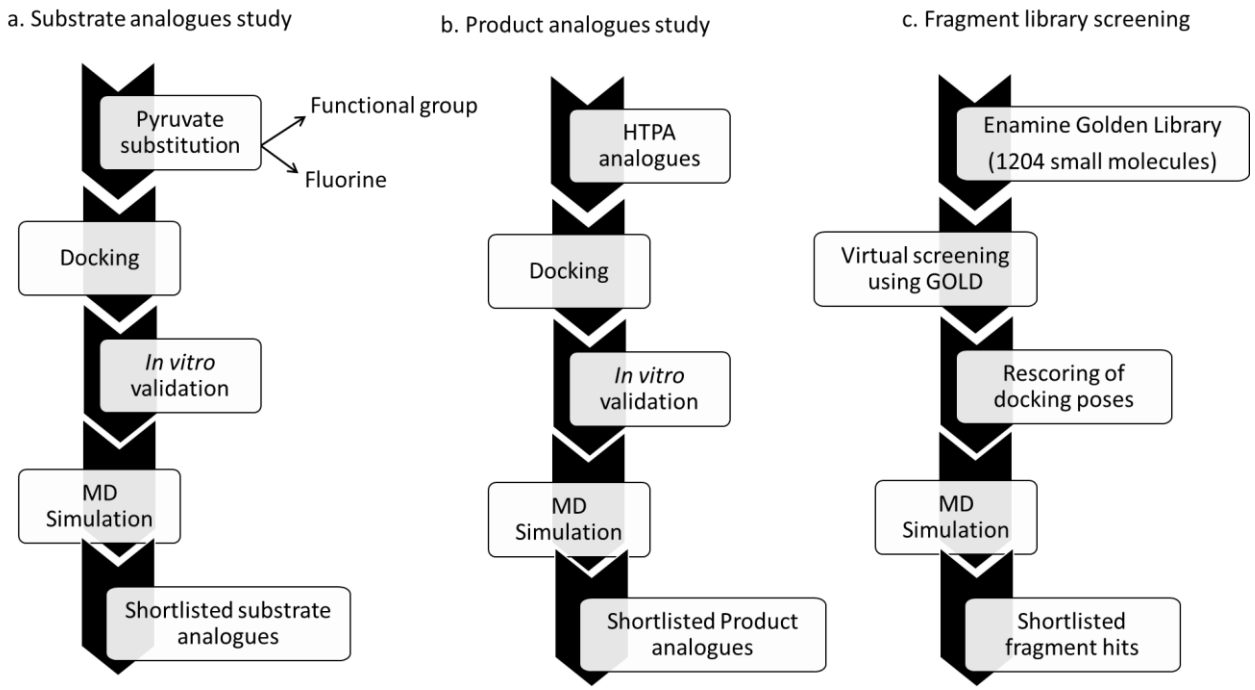

Figure 3: Infographics for workflow (a) Substrate analogue study, (b) Product analogue study and (c) Fragment library screening

Preprints (www.preprints.org) | NOT PEER-REVIEWED | Posted: 25 May 2022 doi:10.20944/preprints202205.0349.v1

2.2 In silico prediction of protein ligand binding

2.2.1 Molecular docking: The starting coordinates for three-dimensional crystal structure of Mtb-DapA (PDB ID: 1XXX and 5J5D) and Mtb-DapB (PDB ID: 1C3V) were retrieved from RCSB Protein Data Bank [25], [26]. For computational studies, only a single chain was selected. Here we have used Autodock Vina [27], Glide [28] and CCDC-GOLD [29] software for docking.

- *Molecular docking using Autodock Vina*: Autodock Vina requires both protein and ligand to be prepared in PDBQT format. The input structure for docking was prepared after removal of water, addition of missing residues and energy minimization using UCSF Chimera [30]. Protein and ligand structures were converted to PDBQT format using MGLTools. The docking grid of 1XXX was constructed with volume of 60 Å × 60 Å × 60 Å centered on the receptor active site amino acid residue Cα of LYS 171, x = 9.785, y = 42.020, z = 69.219. For 1C3V, binding pocket has the volume of 126 Å × 58 Å × 126 Å and centered on the receptor active site amino acid residue NZ of LYS, x = 133.816, y = 24.659 z = 25.207. In both cases default grid point spacing of 0.375 Å was used. Multiple ligands were docked using a batch script. The output gives both binding poses and binding affinities. Binding affinities were extracted using a R script [31] and ligands were shortlisted.
- *Molecular docking using Glide:* The Crystal structure of Dihydrodipicolinate Synthase from *Mycobacterium tuberculosis* in complex with alpha-ketopimelic acid was used for molecular docking using Glide (PDB ID 5J5D)[11]. The structure was optimized using "Protein Preparation wizard" module from Schrödinger Drug Discovery Suite 2017-2. The alpha-ketopimelic acid bound to K171 was removed and this step was followed by one more round of optimization using "Protein Preparation wizard" module. At this step the neutral charge of the K171 side chain of the amine group was set and two water molecules

Preprints (www.preprints.org) | NOT PEER-REVIEWED | Posted: 25 May 2022 doi:10.20944/preprints202205.0349.v1

with hydrogen bonds to alpha-ketopimelic acid ligand were preserved. Screening of the library of small molecules was carried out using Glide software in extra-precision mode using XP scoring function [32].

- *Molecular docking using GOLD:* Virtual screening and rescoring has 4 scoring functions of GOLD (Genetic Optimisation for Ligand Docking) namely, GoldScore, ChemScore, ASP and ChemPLP [33]–[36]. As each scoring function can perform differently with each ligand, so this screening and rescoring method would provide more assertive hits. The binding pocket for docking was selected around reported active site residues of Mtb-DapA. The first step is the virtual screening of the fragment library using all 4 different scoring functions and each run was repeated 3 times. From each score table value, mean and median values were calculated and used as a threshold for selection of compounds for the next rescoring. From each rescoring, consensus fragments were shortlisted for binding analysis.

2.2.2 Binding analysis & selection criteria: The docking poses were analysed for hydrogen bonds using PyMOL [37] and LigPlot [38]. For each case, only ligands forming at least 2 hydrogen bonds with at least one being with active site residue were considered. In the known inhibitor-based approach, we added 2 more criteria prior to visual rescoring as the number of compounds were too high (**Figure 1**). These were (a) analysis of top 3% of docked poses and (b) analysis of docked poses of the compounds with topological polar surface area (tPSA) 91.7Å^2. This tPSA parameter was selected using a regression analysis of a 39-compound dataset from previous work [11]. Regression based statistical modelling was performed by considering different molecular properties like molecular weight, partition coefficient, topological polar surface area, number of hydrogen bond donors and acceptors. This model shows a linear relationship between tPSA and maximum % inhibition with significant P value. We obtained a positive linear relationship with a significant P value (0.00563)

Preprints (www.preprints.org) | NOT PEER-REVIEWED | Posted: 25 May 2022 doi:10.20944/preprints202205.0349.v1

2.3 Molecular dynamic simulation:

The analysis of stability of receptor-ligand complexes was carried out through molecular dynamic simulation using GROMACS version 4.5.5 and 5.1.2 [39]–[41].

Protein topology file was generated using All-atom GROMOS53a6.ff force field [42]. Ligand topologies were generated using PRODRG server [43]. Protein-ligand complexes were neutralized for charges using appropriate number of Na+ ions and wrapped in a periodic box of TIP3P water that was extended to 10 Å from the solvent [44]. Long-range electrostatics and bond lengths within the proteins were restrained using Particle Mesh Ewald method and LINCS algorithm respectively[45], [46]. 1000 steps energy minimization was performed using steepest descent method to ensure that the system has no steric clashes or inappropriate energy. The solvent and ions around the complex were then equilibrated with respect to temperature (300K) and pressure of 1 atmosphere for 100 picosecond (ps) time. Finally, production dynamics was run, and data were collected at every 2 ps time step.

2.3.1 Trajectory analysis

For analysis of trajectories, GROMACS MD simulation toolkit was used. Trajectories of the structure at start and structure at the end of simulation were compared using Root mean squared deviation (RMSD) and per-residue root mean square fluctuation (RMSF). The number of H-bond formed between protein and ligand over time were extracted.

2.4 Cloning, expression and purification

All regular chemicals were of ExelaR grade.

2.4.1 Expression of Mtb-rDapA and Mtb-rDapB: The Mtb-rDapA and Mtb-rDapB open reading frames were cloned in the expression vector pET28a [11]. For the expression of Mtb-rDapA and Mtb-rDapB proteins, recombinant plasmids were transformed into *E. coli* BL21(DE3) and transformants were grown at 37^{o}C in Luria Bertani Broth containing 50µg/ml Kanamycin. At the optical density 0.6, cultures were induced by adding Isopropyl-D-thio-β-

 doi:10.20944/preprints202205.0349.v1

galactopyranoside (IPTG) to a final concentration of 0.75mM for DapA and 0.5mM for DapB and incubation continued with shaking (220 rpm) for 5 hours at 25^{o}C. The cells were harvested by centrifugation at 6000 rpm for 15min at 4^{o}C. The pellet was resuspended in sonication buffer (4ml/100 ml culture) containing 20mM Tris-HCL, pH 7.9, 500mM NaCl, 5mM imidazole, 1mM phenyl methyl sulfonyl fluoride (PMSF), 5%v/v glycerol. Lysozyme was added to the suspension to final concentration of 1mg/ml of sonication buffer and incubated on ice for 30 minutes. Cells were lysed by sonication with 30s pulse and 30s rest on ice for 5 mins followed by centrifugation at 18,000g for 30 min at 4^{o}C. Expressed proteins were soluble in supernatant.

2.4.2 Purification of 6x His-tagged proteins: Purification of Mtb-rDapA and Mtb-rDapB were carried out by affinity chromatography using Nickel-Nitrilotriacetate (Ni-NTA) resin column. Ni-NTA resin column was equilibrated with equilibration buffer (20mM Tris-HCl pH 7.9, 500mM NaCl). Soluble fraction was incubated with 1ml Ni-NTA resin for 2-3 hours at 4℃. The supernatant was loaded on to the column and washed with 25 column volumes of binding buffer (20mM Tris-HCl pH 7.9, 500mM NaCl, 5mM imidazole, 5% v/v glycerol), 15 column volumes of wash buffer-1 (20mM Tris-HCl pH 7.9, 500mM NaCl, 20mM imidazole, 5% v/v glycerol), 15 column volumes of wash buffer-2 (20mM Tris-HCl pH 7.9, 500mM NaCl, 60mM imidazole, 5% v/v glycerol). Elution of bound protein was carried out by elution buffer (20mM Tris-HCl pH 7.9, 500mM NaCl, 250mM imidazole, 5% v/v glycerol). After each step, protein fractions were run on SDS polyacrylamide gel electrophoresis and fractions with clear bands corresponding to the molecular weight of the protein were pooled together. The remaining impurities were removed and concentrated using Amicon ultra concentrator-15 (10kDa NMWL). The concentrations of recombinant proteins were estimated by Bradford method using known concentrations of BSA.

Preprints (www.preprints.org) | NOT PEER-REVIEWED | Posted: 25 May 2022 doi:10.20944/preprints202205.0349.v1

To further confirm identity of purified recombinant proteins, peptide mass fingerprinting was carried out using trypsin and tryptic digested peptides [47]. The 'mass spectra' were searched using Protein Pilot software [48] against protein sequences in the UniProt database [49].

2.5 In-vitro validation using coupled enzymatic assay

To check the inhibition of Mtb-rDapA by shortlisted compound, we have carried out coupled enzymatic assay. We used fixed concentration of pyruvate (500µM), ASA (400µM), Mtb-rDapA (0.2µg/ml) and Mtb-rDapB(3µg/ml) and varied concentrations of compounds. Assay mix was added to each well in a 96 well plate and incubated at 37 °C for 5 min. The reaction was started by the addition of the (S)-ASA. The absorbance at 334 nm was measured at 37 °C (Infinite200PRO spectrophotometer, TECAN) over a time of 3600s (60 min). Water was used as blank, and the negative control contained assay mixture without (S)-ASA. Decrease in absorption commensurate with decreasing concentration of NADPH corresponded to the consumption of substrate, or equivalently, formation of product. The Mtb-rDapB was 16 times in molar excess to ensure complete consumption of dihydrodipicolinate formed. All kinetics measurements were performed in triplicate in 96 well plates. Percentage of inhibition was calculated from the formula, % of inhibition = $\mathbf{([(A_{test(t)} - A_{control(t)})/A_{control(t=0)}]) \times 100}$, **where** $\mathbf{A_{control}}$ is the absorbance of the control sample and Atest is the absorbance of the test sample at 340nm. In the pre-incubation experiments, initially Mtb-rDapA was pre-incubated at 37 °C for 10 min with varying concentrations of the inhibitors. At predetermined time intervals, aliquots were transferred to the standard assay mixture and assayed for enzyme activity.

2.6 Fluorescence based thermal shift assay:

The fluorescence-based thermal shift assay is based on the principle that ligand binding alters thermal stability of protein. This method allows us to monitor the protein denaturation upon heating using fluorescence-based dye (Sypro orange, Sigma, USA), which binds to the hydrophobic part of proteins during protein denaturation and emits fluorescence at 580 nm. We

Preprints (www.preprints.org) | NOT PEER-REVIEWED | Posted: 25 May 2022 doi:10.20944/preprints202205.0349.v1

can monitor the changes in fluorescence and generate a thermal melting curve using a real time PCR machine [50]. The mid-point of the melting curve is designated as the melting temperature (Tm) corresponding to 50% of protein being denatured. The in vitro binding of substrate analogues to Mtb-rDapA and product analogues to Mtb-rDapB were checked by performing a thermal shift assay. The assay mixture was prepared containing 20µM of Mtb-rDapA or Mtb-rDapB, 15X Sypro orange dye, 50mM sodium phosphate buffer pH 7.4 and ligand in 500µM concentration, the thermal scanning was started from 20℃ to 95℃ at heating rate of 0.5℃/min [11], [51].

3. Results:

3.1 *In silico* screening: The compounds shortlisted using different *in silico* approaches are shown in Table 1. The interactive plots of protein and ligand interaction revealed that all shortlisted compounds were predicted to have both polar as well as non-polar interactions with active site residues.

Table 1: Compounds shortlisted using different approaches

Approach	**Compound**	**Binding Residues**
Known inhibitor-based screening	2,6-dioxoheptanedioic acid	**Arg148, Thr54**
	2-oxo-4-pentylpentanedioic acid	Asp196, **Arg148**, Thr55, **Lys171, Gly194**
Substrate analogue study	2-Ketobutyric acid	**Thr54** (2), Leu111, Gly88
	β-Hydroxypyruvic acid	**Thr54**(2)**,** Gly88, Leu111, Val113
	Tartronic acid	**Thr54** (2), Gly88, Leu111, Val113
	α-ketoglutaric acid	**Thr54** (2)
	Tetrafluoropropanoic acid	**Thr54** (2)
	Trifluoropyruvic acid	Gly88 (2), Ser58 (2), **Thr54** (3)
	β-Fluoropyruvic acid	**Thr54** (3)

Preprints (www.preprints.org) | NOT PEER-REVIEWED | Posted: 25 May 2022 doi:10.20944/preprints202205.0349.v1

	4,4,4-triflurobutyric acid	**Thr54** (2), Ser58, Gly88
	5,5,5-Trifluoropentanoic acid	**Thr54**
Fragment library screening	N-(3,4-dihydro-2H-1-benzopyran-4-yl)-1-methyl-1H-pyrazole-4carboxamide	**Arg148**, **Lys171**, Gly194
	3-{[(2-fluorophenyl)methyl]sulfanyl}-6-methyl-4,5-dihydro-1,2,4-triazin-5-one	**Lys171, Arg148, Gly194, Tyr143**
	pyrazolo[1,5-a]pyridine-3-carboxylic acid	**Lys171**, **Arg148**, Thr55, **Tyr143**, **Thr54**
	N-methyl-6-(propan-2-yloxy)pyridine-3-carboxamide	**Lys171**, **Arg148**, **Tyr143**
	N-[(3-fluorophenyl)methyl]-3-methyl-1H-pyrazole-5-carboxamide	**Lys171**, **Arg148**, **Tyr143**
	3-(1-methyl-1H-pyrazol-4-yl)benzoic acid	**Lys171**, **Arg148**, **Tyr143**
	4-cyclobutoxybenzoic acid	**Lys171**, **Tyr143**, **Arg148**, Gly256, Val257
Product analogue study	2,6-Pyridine dicarboxylic acid	Thr577, Lys636, Thr643, His632

a) Known inhibitor-based screening: PubChem library was screened initially for ≥90% followed by ≥70% structure similarity to αKPA. In the initial search 26 compounds were retrieved all of which were subjected to binding pose analysis using molecular docking approach. During analysis, 10 compounds were found to be interacting with Mtb-DapA active site residues (Suppl Table S1). Further, during extended PubChem search with ≥70% structure similarity, 5615 compounds were obtained. As described in the methodology section, 2 criteria were set for binding analysis. The first criterion was based on estimation of the independent molecular docking scoring function (Autodock Score), as lower the score, better the predicted stability. Through this criteria, 152 top hits were selected for protein ligand interaction analysis and among them 21 were found to form 2 or more hydrogen bond with Mtb-DapA and at least one

 doi:10.20944/preprints202205.0349.v1

of them was with active site residues (Suppl Table S2). Further, next criterion was to screen compounds with tPSA 91.7 Å2 from our docked set. From the compound dataset, 129 docked compounds with required tPSA were taken out for analysis. After visualization of hydrogen bond interaction, 46 compounds were shortlisted (Suppl Table S3). Additionally, 48 compounds with ≥90% structure similarity to αKPA were gathered from ZINC database. After molecular docking using Autodock Vina, 4 of them were found to forming interactions with Mtb-DapA active site (Suppl Table S4). These compounds were selected for further studies. Molecular dynamic simulation was performed for all the above listed compounds (Suppl Table S1, S2, S3 and S4). Initially MDS was performed for 10ns of time and trajectories and hydrogen bonds were visualized. Further, simulation was extended till 40ns only for those compounds wherever stable protein-ligand interaction was observed. Following that stability of interaction was inspected again through trajectory analysis. Total 11 compounds were shortlisted after molecular docking and molecular dynamic simulation. Subsequently, cross validation or complementary evaluation was carried out for these 11 compounds (Suppl Table S5). For that the binding score, as estimated by XP score, Mtb-DapA inhibitor with reported IC50 values were taken as control set. Binding scores were compared with that of the 11 shortlisted compounds. It can be observed from control dataset of Suppl Table S5 that 2-oxohexanedioic acid had the lowest XP score (-8.7216) followed by αKPA (-8.69031). Among them αKPA was a validated Mtb-rDaA inhibitor with the maximum percentage inhibition 88% [27]. The comparable binding scores were observed for 2 compounds from the test dataset (shortlisted compounds), 2-oxo-4-pentylpentanedioic acid (XP score: -8.78965) and 2,6-dioxoheptanedioic acid (XP score: -8.48284). Following this observation, these 2 compounds were shortlisted as highly potent lead molecules against Mtb-DapA. Finally, 2,6-dioxoheptanedioic acid

 doi:10.20944/preprints202205.0349.v1

and 2-oxo-4-pentylpentanedioic acid were shortlisted as hits. The hydrogen bond pattern between ligands and Mtb-dapA was analyzed from MD simulation results. The binding to at least one active site residue is considered for positive scoring. The binding between compounds and the active site of Mtb-dapA and hydrogen bond patterns are shown in Figure 4.

b) Substrate analogue study: Substrate analogues were designed by substituting various functional groups and fluorine at different positions. The binding score of these compounds were predicted to be lower than that of pyruvate (AutoDock XP score: -3.6 kcal/mol), which is the natural substrate for Mtb-DapA. Further, interacting residues were examined by LigPlot+ v.2.2.4[38]. The shortlisted substrate analogues and their interacting residues of Mtb-DapA are shown in Table 1. The list contains 4 pyruvate analogues, 3 fluorine substituted pyruvate analogues and 2 fluorine substituted KPA analogues. All of them were predicted to interact with Thr54 of Mtb-DapA active site.

c) Product analogue study: In the first 2 approaches, we have overwhelmingly focused on designing substrate analogues and we were able to select some of the small molecules as hits. Unlike that, in this last approach we have rather focused on (4S)- 4- hydroxy – 2,3, 4, 5 tetrahydro –(2S)- dipicolinate (HTPA), the product formed in condensation reaction catalyzed by Mtb-DapA enzyme. Previous studies have also reported Dipolinic acid as a competitive inhibitor of E. coli DapA [25]. For this work, compounds were screened from Sigma Aldrich Chemical library and docked against Mtb-DapB. The crystal structure of Mtb-DapB (PDB ID: 1C3V) was solved in complex with NADPH and Dipicolinic acid. Dipicolinic acid and 3 other compounds namely, 6-(Hydroxymethyl)picolinic acid, 2-Picolinic acid and Chelidonic acid were selected for docking. Among them Dipicolinic acid had the lowest binding score and rest 3

Preprints (www.preprints.org) | NOT PEER-REVIEWED | Posted: 25 May 2022 doi:10.20944/preprints202205.0349.v1

compounds had binding score higher than this compound. Therefore, these compounds were excluded from further studies.

d) Fragment library screening: Using a stringent computational approach of virtual screening and rescoring, 7 compounds were shortlisted from Enamine Fragment library. The score distribution in virtual screening and rescoring is shown in Figure 5. The consensus compounds shortlisted as hits are listed in **Table 1** along with the interacting residues from Mtb-DapA active sites. The reported active site residues Thr55, Arg148, Tyr143 and Lys171 (catalytic) were observed to participate in ligand binding. Further, MD simulation showed stable hydrogen bond patterns **(Figure: 6a)** of the shortlisted compounds with Mtb-DapA. The RMSD of these compounds **(Figure: 6b)** were also comparable to that of the apo-protein.

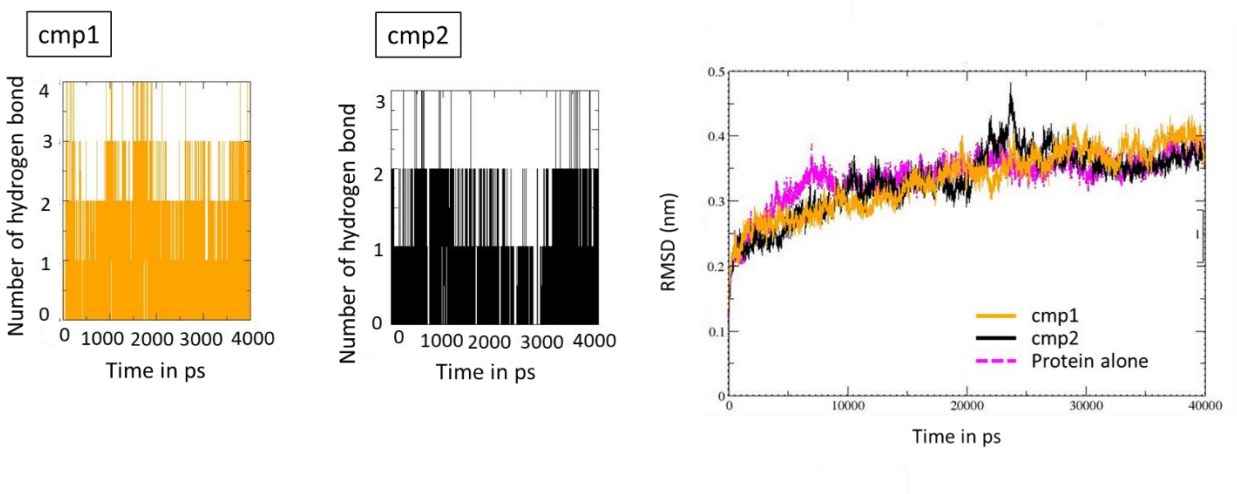

Figure 4: Hydrogen bond and RMSD plot of compounds selected using known inhibitor-based screening. Here, cmp1: 2,6-dioxoheptanedioic acid, cmp2: 2-oxo-4-pentylpentanedioic acid

Preprints (www.preprints.org) | NOT PEER-REVIEWED | Posted: 25 May 2022 doi:10.20944/preprints202205.0349.v1

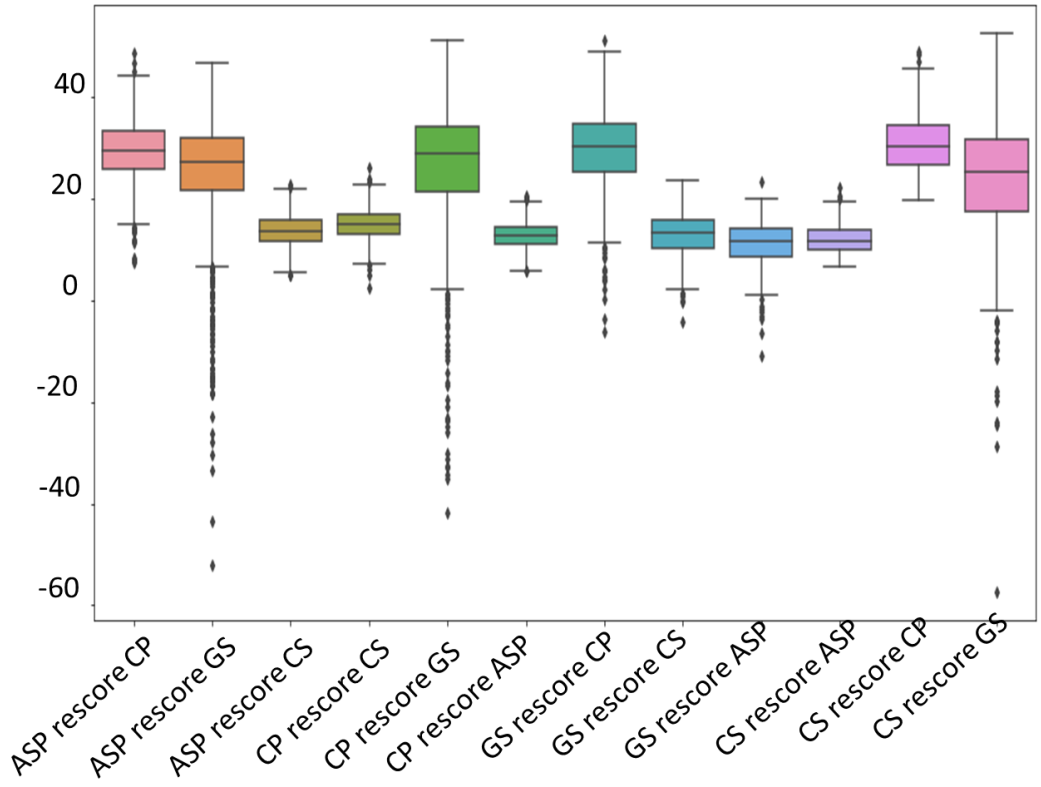

Figure 5: Boxplot showing score distribution after virtual screening and rescoring using CCDC-GOLD.

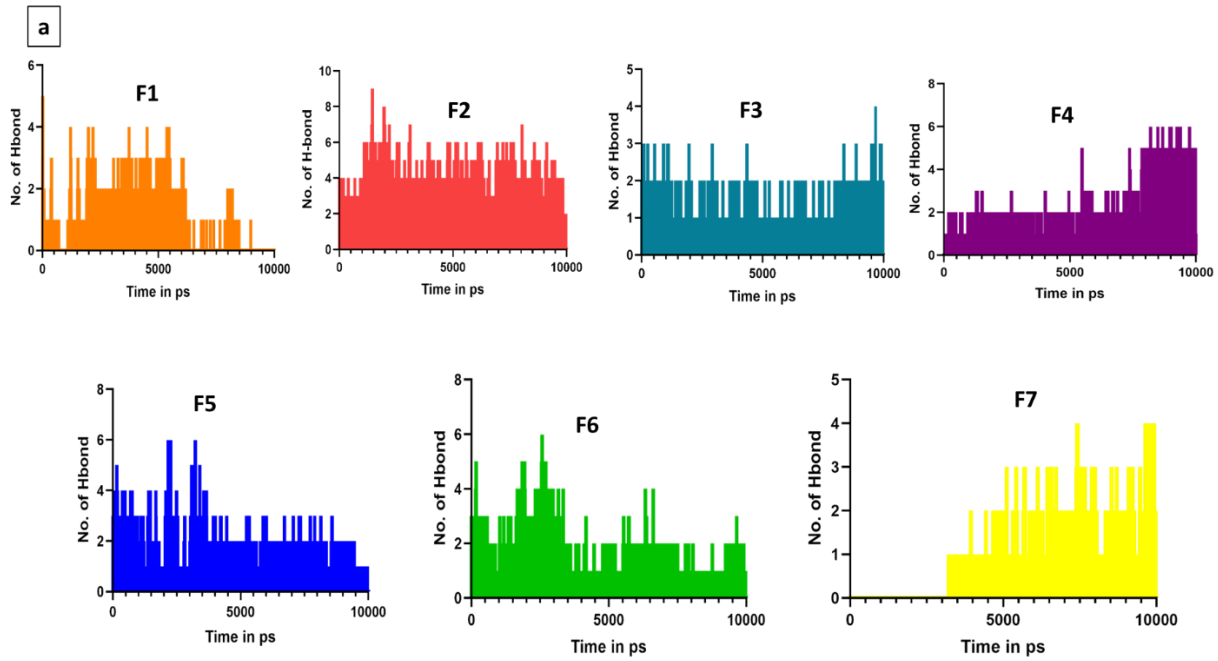

Preprints (www.preprints.org) | NOT PEER-REVIEWED | Posted: 25 May 2022 doi:10.20944/preprints202205.0349.v1

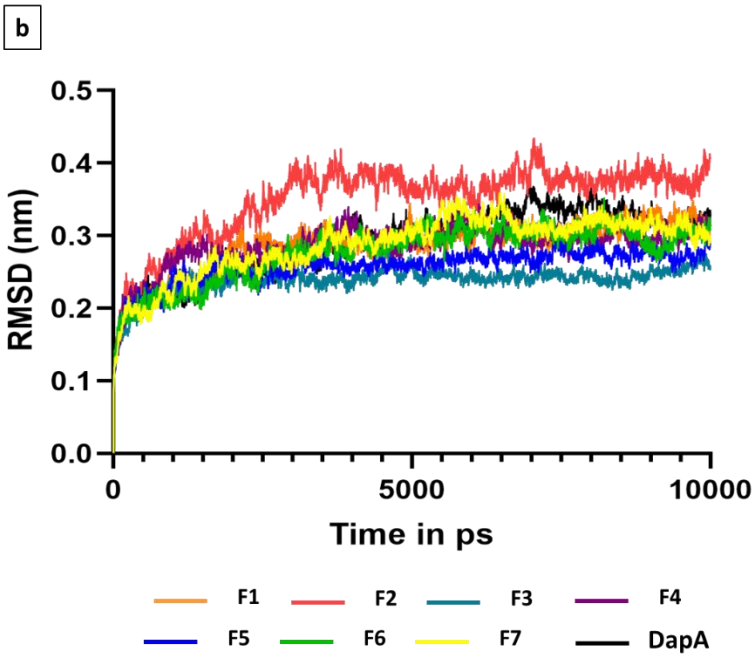

Figure 6: Molecular Dynamic simulation of compounds from fragment library screening. (a)Hydrogen bond plot, (b) Root mean squared deviation (RMSD) after 10ns of simulation.

3.2 In-vitro validation of shortlisted compounds:

a) Coupled enzymatic assay

HTPA is reduced to THDP whereby NADPH gets oxidized to NADP+, which can be measured by the decrease in absorbance at 334 nm. Inhibition of either Mtb-rDapA or Mtb-rDapB would inhibit the oxidation of NADPH. The shortlisted substrate and product analogues were validated using this *in vitro* assay. The maximum percentage inhibition at 500µM is listed in **Table 2**. Unfortunately, due to unavailability, the compounds shortlisted using known inhibitor-based approach and fragment library screening could not be validated further.

Preprints (www.preprints.org) | NOT PEER-REVIEWED | Posted: 25 May 2022 doi:10.20944/preprints202205.0349.v1

Among the tested compounds, β-hydroxy pyruvic acid and Tartronic acid exhibited inhibitions at concentration as low as 50µM **(Figure 7)**. These 2 compounds were shortlisted as potent inhibitors of Mtb-rDapA**.**

β-hydroxy pyruvic acid exhibits a time dependent inhibition against *E. coli* dapA [52]. Time dependent inhibition is observed when inhibition proportionately increases with the pre-incubation time. This is due to slow binding of enzyme and inhibitor followed by the formation of tight enzyme inhibitor complex [53]. The inhibitory activity against Mtb-rDapA increases from 18% to 48% by increasing the pre-incubation time from 10 min to 30 min (**Figure 8**).

Table 2: Maximum percentage inhibition against Mtb-rDapA at 500µM

ID	IUPAC Name	Maximum Inhibition (%)
C1	2-Ketobutyric acid	3.12
C2	β-Hydroxypyruvic acid	48.7
C4	6-Hydroxymethyl-pyridine-2-carboxylic acid	34.8
C5	2-Picolinic acid/ Pyridine-2-carboxylic acid	31.22
C7	α-ketoglutaric acid	0.38
C8	4,4,4-triflurobutyric acid	28.22
C10	4H-Pyran-2,6-dicarboxylic Acid	21.87
C11	pyridine-2,6-dicarboxylic acid	21.75
C13	5,5,5-Trifluoropentanoic acid	30.75
C14	Tetrafluoropropanoic acid	43.8
C15	Trifluoropyruvic acid	6.54
C16	Tartronic acid	51.55
C17	β-Fluoropyruvic acid	13.4

 doi:10.20944/preprints202205.0349.v1

b) Thermal shift assay

The fluorescence based thermal shift assay was performed for screening of identified ligands, which is based on the principle that ligand binding alters thermal stability of protein. Here sypro orange dye is used, which binds to hydrophobic parts of proteins and emits fluorescence during protein denaturation. The Tm of Mtb-rDapA increased by 2 °C upon binding pyruvate, and by 3 °C upon binding to 500µM β-hydroxypyruvic acid. Again, upon binding of 2,6-Pyridine dicarboxylic acid at same concentration, Tm of Mtb-rDapB changes by 0.5˚C (**Figure 9**).

c) Combination of inhibitors:

This approach was designed by combining validated substrate and product analogues as none of the shortlisted inhibitors were very potent. Various concentrations of substrate (α-Ketopimelic acid, Tartronic acid) and product analogues (2,6-Pyridine dicarboxylic acid) were used. It was observed that, the percentage inhibition increased to nearly 100% when coupled assay was performed by combination of 20 µM α-Ketopimelic acid with 200 µM 2,6-Pyridine dicarboxylic acid and 50 µM Tartronic acid with 200 µM 2,6-Pyridine dicarboxylic acid (**Figure 10**).

Preprints (www.preprints.org) | NOT PEER-REVIEWED | Posted: 25 May 2022 doi:10.20944/preprints202205.0349.v1

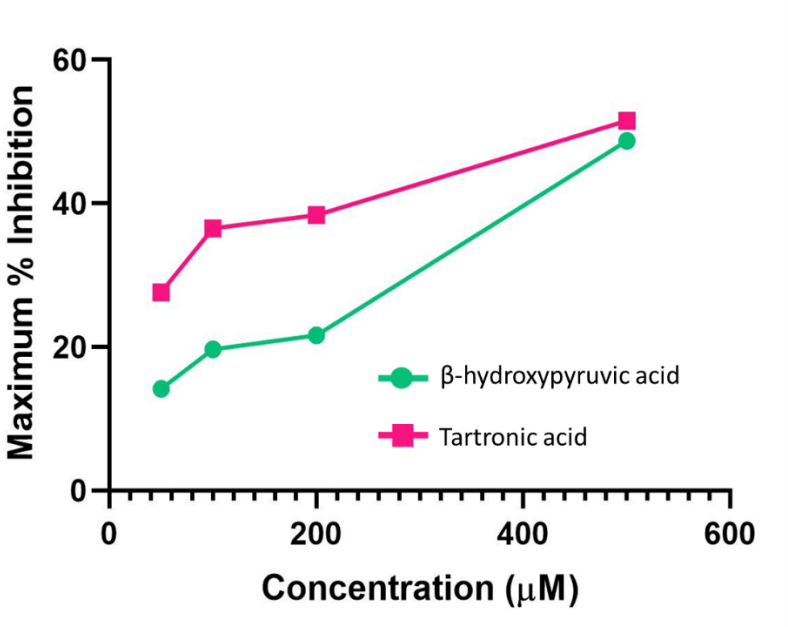

Figure 7: Maximum inhibition (%) showed by, β-hydroxy pyruvic acid and Tartronic acid at various concentrations

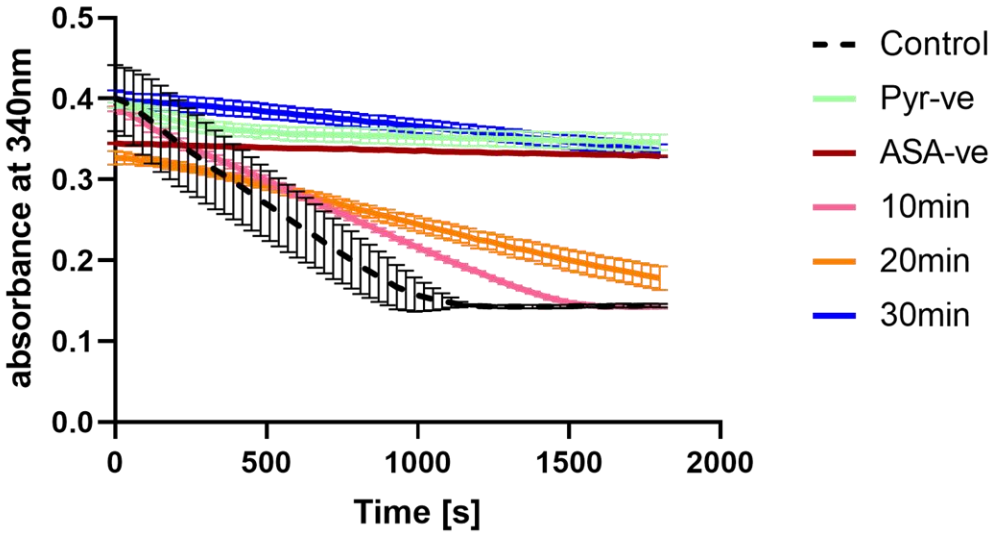

Figure 8: Time dependent activity of β-hydroxy pyruvic acid against Mtb-rDapA at 200μM

Preprints (www.preprints.org) | NOT PEER-REVIEWED | Posted: 25 May 2022 doi:10.20944/preprints202205.0349.v1

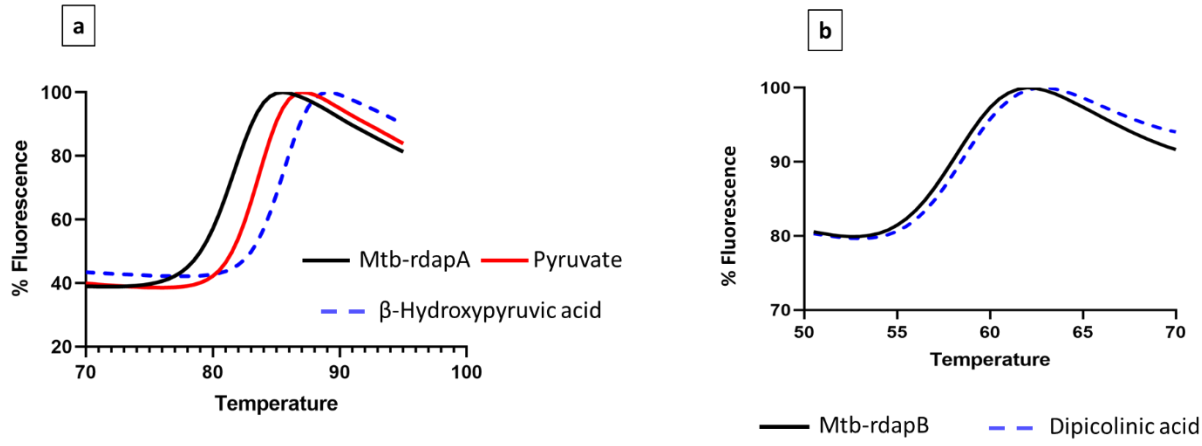

Figure 9: Thermal shift assay of (a) substrate analogues with Mtb-rDapA and (b) product analogues with Mtb-rDapB

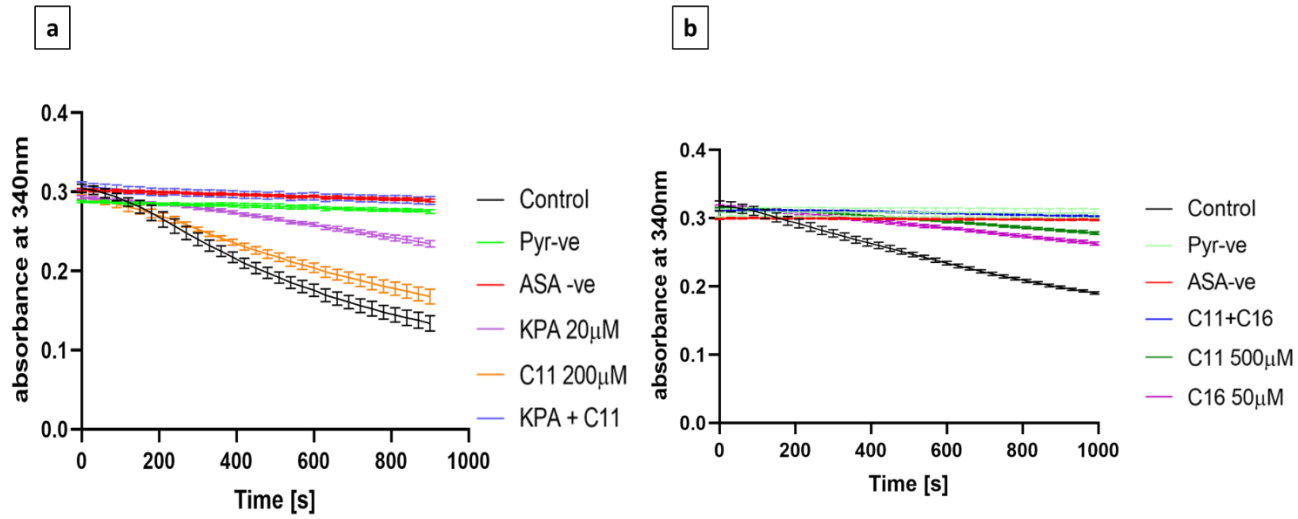

Figure 10: Coupled assay using (a) α-KPA at 20µM + 2,6-Pyridine dicarboxylic acid (C11) at 200µM and (b) Tartronic acid at 50µM + 2,6-Pyridine dicarboxylic acid (C11) at 500µM

3.3 MD simulation of final shortlisted inhibitors

To computationally examine the results of *in vitro* assay, MD simulation was performed. The interaction stability of Mtb-DapA+β-hydroxypyruvic acid, Mtb-DapA+Tartronic acid and Mtb-DapB+2,6-Pyridine dicarboxylic acid were studied. MD simulation predicted stable interaction over time **(Figure 11)**.

Preprints (www.preprints.org) | NOT PEER-REVIEWED | Posted: 25 May 2022 doi:10.20944/preprints202205.0349.v1

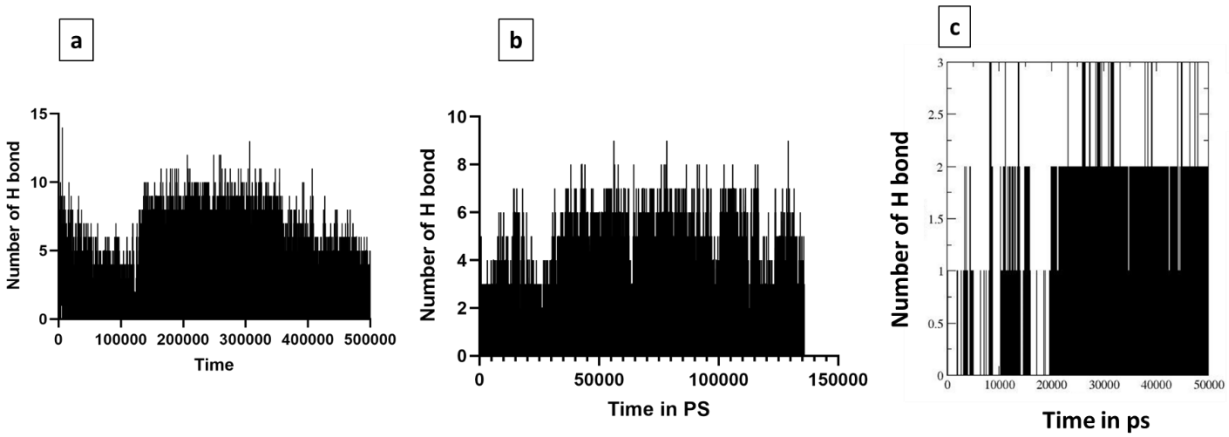

Figure 11: MD Simulation of shortlisted compounds, (a) β-hydroxypyruvic acid, (b) Tartronic acid and (c) 2,6-Pyridine dicarboxylic acid

4. Discussion

The *M. tuberculosis* DAP enzyme, Mtb-DapA and Mtb-DapB are potential drug targets with large avenues for identification of novel inhibitors. Several attempts, both *in silico* and *in vitro* were carried out for identification of potent inhibitors. α-KPA is one such validated Mtb-rDapA inhibitor of IC_{50} 21µM with 88% maximum inhibition [11]. In this study, we have identified and validated potent inhibitors with activity against Mtb-DapA using novel approaches.

In silico screening predicted 2 structure analogues of α-KPA, 2,6-dioxoheptanedioic acid and 2-oxo-4-pentylpentanedioic acid as Mtb-DapA inhibitors. These compounds were predicted to interact with the active site Arg148 and Thr54 with the better binding scores compared to known inhibitor α-KPA. 2-oxo-4-pentylpentanedioic acid even showed hydrogen bonding with catalytic residue Lys171. Further, 7 leads were shortlisted using fragment library screening. All the 7 compounds were predicted to interact with several active site residues of Mtb-DapA, namely Arg148, Thr54, Tyr143 as well as with Lys171. Molecular dynamic simulations showed that the interactions were stable over time. Unfortunately, these compounds were not validated *in vitro* due to commercial unavailability.

 doi:10.20944/preprints202205.0349.v1

In vitro studies revealed that substrate analogues, β-hydroxypyruvic acid tartronic acid are inhibitors of Mtb-rDapA with maximum inhibition 48% and 51% at 500µM concentrations respectively. Earlier, Dobson et al., had reported β-hydroxypyruvic acid as a time dependent inhibitor of *E. coli* DapA enzyme. The time dependent inhibition is observed due to slow binding of enzyme and inhibitor followed by formation of tight enzyme inhibitor complex with increased pre-incubation time. We have examined this observation in Mtb-rDapA as inhibition by this compound at 200µM increased from 18% to 48% when pre incubation time was increased from 10 min to 30 min. Further, TSA showed that β-hydroxypyruvic acid interacts with Mtb-rDapA as the thermal stability of Mtb-rDapA shifted by 3˚C in presence of this compound. Among the product analogues of Mtb-DapA, dipicolinic acid showed to bind to Mtb-rDapB. The thermal stability of Mtb-rDapB shifted by 0.5˚C in binding with dipicolinic acid. Additionally, we have designed a new approach by combining substrate and product analogues to achieve better inhibitions. *In vitro* assays validated that this combination approach increased maximum inhibition up to 100% showed by known inhibitor α-KPA and new inhibitors tartronic acid identified in this study in combination with dipicolinic acid. Therefore, the following conclusions can be drawn from this study:

- Inhibitors of Mtb-DapA were identified using *in silico* and *in vitro* screening.
- The in vitro validated compounds were carboxylic acids with hydroxyl group at alpha position and these had satisfied previous rules [11].
- Combination of substrate and product analogues inhibitors can be an alternative strategy to increase potency.

References:

[1] "Global tuberculosis report 2021." https://www.who.int/publications-detail-redirect/9789240037021 (accessed May 18, 2022).

[2] L. J. Alderwick, J. Harrison, G. S. Lloyd, and H. L. Birch, "The Mycobacterial Cell Wall--Peptidoglycan and Arabinogalactan," *Cold Spring Harb. Perspect. Med.*, vol. 5, no. 8, p. a021113, Mar. 2015, doi: 10.1101/cshperspect.a021113.

[3] S. Mahapatra, D. C. Crick, and P. J. Brennan, “Comparison of the UDP-N-acetylmuramate:L-alanine ligase enzymes from Mycobacterium tuberculosis and Mycobacterium leprae,” *J. Bacteriol.*, vol. 182, no. 23, pp. 6827–6830, Dec. 2000, doi: 10.1128/JB.182.23.6827-6830.2000.

[4] J. B. Raymond, S. Mahapatra, D. C. Crick, and M. S. Pavelka, “Identification of the namH gene, encoding the hydroxylase responsible for the N-glycolylation of the mycobacterial peptidoglycan,” *J. Biol. Chem.*, vol. 280, no. 1, pp. 326–333, Jan. 2005, doi: 10.1074/jbc.M411006200.

[5] S. Mahapatra, H. Scherman, P. J. Brennan, and D. C. Crick, “N Glycolylation of the nucleotide precursors of peptidoglycan biosynthesis of Mycobacterium spp. is altered by drug treatment,” *J. Bacteriol.*, vol. 187, no. 7, pp. 2341–2347, Apr. 2005, doi: 10.1128/JB.187.7.2341-2347.2005.

[6] Y. Minato *et al.*, “Genomewide Assessment of Mycobacterium tuberculosis Conditionally Essential Metabolic Pathways,” *mSystems*, vol. 4, no. 4, pp. e00070-19, doi: 10.1128/mSystems.00070-19.

[7] M. S. Pavelka and W. R. Jacobs, “Biosynthesis of diaminopimelate, the precursor of lysine and a component of peptidoglycan, is an essential function of Mycobacterium smegmatis,” *J. Bacteriol.*, vol. 178, no. 22, pp. 6496–6507, Nov. 1996, doi: 10.1128/jb.178.22.6496-6507.1996.

[8] G. Kefala *et al.*, “Crystal structure and kinetic study of dihydrodipicolinate synthase from Mycobacterium tuberculosis,” *Biochem. J.*, vol. 411, no. 2, pp. 351–360, Apr. 2008, doi: 10.1042/BJ20071360.

[9] M. Cirilli, R. Zheng, G. Scapin, and J. S. Blanchard, “The three-dimensional structures of the Mycobacterium tuberculosis dihydrodipicolinate reductase-NADH-2,6-PDC and -NADPH-2,6-PDC complexes. Structural and mutagenic analysis of relaxed nucleotide specificity,” *Biochemistry*, vol. 42, no. 36, pp. 10644–10650, Sep. 2003, doi: 10.1021/bi030044v.

[10] V. Mitsakos *et al.*, “Inhibiting dihydrodipicolinate synthase across species: towards specificity for pathogens?,” *Bioorg. Med. Chem. Lett.*, vol. 18, no. 2, pp. 842–844, Jan. 2008, doi: 10.1016/j.bmcl.2007.11.026.

[11] P. Shrivastava *et al.*, “Inhibition of Mycobacterium tuberculosis dihydrodipicolinate synthase by alpha-ketopimelic acid and its other structural analogues,” *Sci. Rep.*, vol. 6, p. 30827, Aug. 2016, doi: 10.1038/srep30827.

[12] A. Rehman *et al.*, “Identification of potential leads against 4-hydroxytetrahydrodipicolinate synthase from Mycobacterium tuberculosis,” *Bioinformation*, vol. 12, no. 11, pp. 400–407, 2016, doi: 10.6026/97320630012400.

[13] A. Garg, R. Tewari, and G. P. Raghava, “Virtual Screening of potential drug-like inhibitors against Lysine/DAP pathway of Mycobacterium tuberculosis,” *BMC Bioinformatics*, vol. 11, no. 1, p. S53, Jan. 2010, doi: 10.1186/1471-2105-11-S1-S53.

[14] “Dihydrodipicolinate Synthase from Escherichia coli: pH Dependent Changes in the Kinetic Mechanism and Kinetic Mechanism of Allosteric Inhibition by l-Lysine | Biochemistry.” https://pubs.acs.org/doi/abs/10.1021/bi962264x (accessed Feb. 24, 2022).

[15] B. A. Boughton, R. C. J. Dobson, J. A. Gerrard, and C. A. Hutton, “Conformationally constrained diketopimelic acid analogues as inhibitors of dihydrodipicolinate synthase,” *Bioorg. Med. Chem. Lett.*, vol. 18, no. 2, pp. 460–463, Jan. 2008, doi: 10.1016/j.bmcl.2007.11.108.

[16] C. V. Coulter, J. A. Gerrard, J. A. E. Kraunsoe, and A. J. Pratt, “Escherichia coli dihydrodipicolinate synthase and dihydrodipicolinate reductase: kinetic and inhibition studies of two putative herbicide targets,” *Pestic. Sci.*, vol. 55, no. 9, pp. 887–895, 1999, doi: 10.1002/(SICI)1096-9063(199909)55:9<887::AID-PS36>3.0.CO;2-B.

[17] “Pyridine and piperidine derivatives as inhibitors of dihydrodipicolinic acid synthase, a key enzyme in the diaminopimelate pathway to l-lysine - ScienceDirect.” https://www.sciencedirect.com/science/article/abs/pii/0960894X94850232 (accessed Feb. 24, 2022).

[18] J. J. Turner, J. P. Healy, R. C. J. Dobson, J. A. Gerrard, and C. A. Hutton, “Two new irreversible inhibitors of dihydrodipicolinate synthase: diethyl (E,E)-4-oxo-2,5-heptadienedioate and diethyl

(E)-4-oxo-2-heptenedioate," *Bioorg. Med. Chem. Lett.*, vol. 15, no. 4, pp. 995–998, Feb. 2005, doi: 10.1016/j.bmcl.2004.12.043.

[19] X. Yan, C. Liao, Z. Liu, A. T. Hagler, Q. Gu, and J. Xu, "Chemical Structure Similarity Search for Ligand-based Virtual Screening: Methods and Computational Resources," *Curr. Drug Targets*, vol. 17, no. 14, pp. 1580–1585, 2016, doi: 10.2174/1389450116666151102095555.

[20] S. Kim *et al.*, "PubChem in 2021: new data content and improved web interfaces," *Nucleic Acids Res.*, vol. 49, no. D1, pp. D1388–D1395, Jan. 2021, doi: 10.1093/nar/gkaa971.

[21] J. J. Irwin and B. K. Shoichet, "ZINC − A Free Database of Commercially Available Compounds for Virtual Screening," *J. Chem. Inf. Model.*, vol. 45, no. 1, pp. 177–182, Jan. 2005, doi: 10.1021/ci049714+.

[22] R. E. Lenga, "The Sigma-Aldrich library of chemical safety data," Sigma-Aldrich Corp., 1988. Accessed: May 18, 2022. [Online]. Available: https://scholar.google.com/scholar_lookup?title=The+Sigma-Aldrich+library+of+chemical+safety+data&author=Lenga%2C+R.E.&publication_year=1988

[23] O. O. Grygorenko, "Enamine Ltd.: The Science and Business of Organic Chemistry and Beyond," *Eur. J. Org. Chem.*, vol. 2021, no. 47, pp. 6474–6477, 2021, doi: 10.1002/ejoc.202101210.

[24] "The RDKit Documentation — The RDKit 2021.09.1 documentation." https://www.rdkit.org/docs/ (accessed Feb. 24, 2022).

[25] R. P. D. Bank, "RCSB PDB: Homepage." https://www.rcsb.org/ (accessed May 16, 2022).

[26] H. Berman, K. Henrick, and H. Nakamura, "Announcing the worldwide Protein Data Bank," *Nat. Struct. Mol. Biol.*, vol. 10, no. 12, Art. no. 12, Dec. 2003, doi: 10.1038/nsb1203-980.

[27] O. Trott and A. J. Olson, "AutoDock Vina: Improving the speed and accuracy of docking with a new scoring function, efficient optimization, and multithreading," *J. Comput. Chem.*, vol. 31, no. 2, pp. 455–461, 2010, doi: 10.1002/jcc.21334.

[28] R. A. Friesner *et al.*, "Glide: A New Approach for Rapid, Accurate Docking and Scoring. 1. Method and Assessment of Docking Accuracy," *J. Med. Chem.*, vol. 47, no. 7, pp. 1739–1749, Mar. 2004, doi: 10.1021/jm0306430.

[29] G. Jones, P. Willett, R. C. Glen, A. R. Leach, and R. Taylor, "Development and validation of a genetic algorithm for flexible docking11Edited by F. E. Cohen," *J. Mol. Biol.*, vol. 267, no. 3, pp. 727–748, Apr. 1997, doi: 10.1006/jmbi.1996.0897.

[30] "UCSF Chimera—A visualization system for exploratory research and analysis - Pettersen - 2004 - Journal of Computational Chemistry - Wiley Online Library." https://onlinelibrary.wiley.com/doi/full/10.1002/jcc.20084 (accessed May 16, 2022).

[31] "R Core Team (2013). R: A language and environment for statistical computing. R Foundation for Statistical Computing, Vienna, Austria. URL http://www.R-project.org/".

[32] "Extra Precision Glide: Docking and Scoring Incorporating a Model of Hydrophobic Enclosure for Protein−Ligand Complexes | Journal of Medicinal Chemistry." https://pubs.acs.org/doi/abs/10.1021/jm051256o (accessed Feb. 24, 2022).

[33] M. D. Eldridge, C. W. Murray, T. R. Auton, G. V. Paolini, and R. P. Mee, "Empirical scoring functions: I. The development of a fast empirical scoring function to estimate the binding affinity of ligands in receptor complexes," *J. Comput. Aided Mol. Des.*, vol. 11, no. 5, pp. 425–445, Sep. 1997, doi: 10.1023/A:1007996124545.

[34] C. A. Baxter, C. W. Murray, D. E. Clark, D. R. Westhead, and M. D. Eldridge, "Flexible docking using tabu search and an empirical estimate of binding affinity," *Proteins Struct. Funct. Bioinforma.*, vol. 33, no. 3, pp. 367–382, 1998, doi: 10.1002/(SICI)1097-0134(19981115)33:3<367::AID-PROT6>3.0.CO;2-W.

[35] W. T. M. Mooij and M. L. Verdonk, "General and targeted statistical potentials for protein–ligand interactions," *Proteins Struct. Funct. Bioinforma.*, vol. 61, no. 2, pp. 272–287, 2005, doi: 10.1002/prot.20588.

[36] O. Korb, T. Stützle, and T. E. Exner, "Empirical scoring functions for advanced protein-ligand docking with PLANTS," *J. Chem. Inf. Model.*, vol. 49, no. 1, pp. 84–96, Jan. 2009, doi: 10.1021/ci800298z.
[37] "PyMOL | pymol.org." https://pymol.org/2/ (accessed May 16, 2022).
[38] R. A. Laskowski and M. B. Swindells, "LigPlot+: multiple ligand-protein interaction diagrams for drug discovery," *J. Chem. Inf. Model.*, vol. 51, no. 10, pp. 2778–2786, Oct. 2011, doi: 10.1021/ci200227u.
[39] H. BEKKER *et al.*, "GROMACS - A PARALLEL COMPUTER FOR MOLECULAR-DYNAMICS SIMULATIONS: 4th International Conference on Computational Physics (PC 92)," *Phys. Comput. 92*, pp. 252–256, 1993.
[40] "GROMACS 4.5: a high-throughput and highly parallel open source molecular simulation toolkit | Bioinformatics | Oxford Academic." https://academic.oup.com/bioinformatics/article/29/7/845/253065?login=true (accessed Feb. 24, 2022).
[41] M. J. Abraham *et al.*, "GROMACS: High performance molecular simulations through multi-level parallelism from laptops to supercomputers," *SoftwareX*, vol. 1–2, pp. 19–25, Sep. 2015, doi: 10.1016/j.softx.2015.06.001.
[42] C. Oostenbrink, A. Villa, A. E. Mark, and W. F. van Gunsteren, "A biomolecular force field based on the free enthalpy of hydration and solvation: the GROMOS force-field parameter sets 53A5 and 53A6," *J. Comput. Chem.*, vol. 25, no. 13, pp. 1656–1676, Oct. 2004, doi: 10.1002/jcc.20090.
[43] A. W. Schüttelkopf and D. M. F. van Aalten, "PRODRG: a tool for high-throughput crystallography of protein-ligand complexes," *Acta Crystallogr. D Biol. Crystallogr.*, vol. 60, no. Pt 8, pp. 1355–1363, Aug. 2004, doi: 10.1107/S0907444904011679.
[44] Y. Duan *et al.*, "A point-charge force field for molecular mechanics simulations of proteins based on condensed-phase quantum mechanical calculations," *J. Comput. Chem.*, vol. 24, no. 16, pp. 1999–2012, Dec. 2003, doi: 10.1002/jcc.10349.
[45] T. Darden, D. York, and L. Pedersen, "Particle mesh Ewald: An N·log(N) method for Ewald sums in large systems," *J. Chem. Phys.*, vol. 98, no. 12, pp. 10089–10092, Jun. 1993, doi: 10.1063/1.464397.
[46] B. Hess, H. Bekker, H. J. C. Berendsen, and J. G. E. M. Fraaije, "LINCS: A linear constraint solver for molecular simulations," *J. Comput. Chem.*, vol. 18, no. 12, pp. 1463–1472, 1997, doi: 10.1002/(SICI)1096-987X(199709)18:12<1463::AID-JCC4>3.0.CO;2-H.
[47] B. Thiede *et al.*, "Peptide mass fingerprinting," *Methods San Diego Calif*, vol. 35, no. 3, pp. 237–247, Mar. 2005, doi: 10.1016/j.ymeth.2004.08.015.
[48] "Seymour, S. L., & Hunter, C. L. (2015). ProteinPilot™ Software Overview. In High quality, in-depth protein identification and protein expression analysis.".
[49] The UniProt Consortium, "UniProt: the universal protein knowledgebase in 2021," *Nucleic Acids Res.*, vol. 49, no. D1, pp. D480–D489, Jan. 2021, doi: 10.1093/nar/gkaa1100.
[50] F. H. Niesen, H. Berglund, and M. Vedadi, "The use of differential scanning fluorimetry to detect ligand interactions that promote protein stability," *Nat. Protoc.*, vol. 2, no. 9, pp. 2212–2221, 2007, doi: 10.1038/nprot.2007.321.
[51] S. N. Krishna *et al.*, "A fluorescence-based thermal shift assay identifies inhibitors of mitogen activated protein kinase kinase 4," *PloS One*, vol. 8, no. 12, p. e81504, 2013, doi: 10.1371/journal.pone.0081504.
[52] R. C. J. Dobson *et al.*, "Conserved main-chain peptide distortions: A proposed role for Ile203 in catalysis by dihydrodipicolinate synthase," *Protein Sci.*, vol. 17, no. 12, pp. 2080–2090, 2008, doi: 10.1110/ps.037440.108.
[53] L. Cheng, T. K. H. Chang, and H. Wong, "Drug-Drug Interactions With a Pharmacokinetic Basis," in *Reference Module in Biomedical Sciences*, Elsevier, 2021. doi: 10.1016/B978-0-12-820472-6.00179-1.

 doi:10.20944/preprints202205.0349.v1

Statements and Declarations

Funding statement

SR's work is supported in part by a grant from ICMR (No. BIC/5(09)/Indo-Russian/2016). AB acknowledges DBT and British Council for Newton Bhabha Fellowship (F.No. BT/IN/UK/DBT-BC/2018-2019).

Acknowledgement:

Authors acknowledge Dr. Jyoti Rani for valuable support and feedback. AB and PC acknowledges UGC for fellowship. The molecular dynamics simulations were carried out in the super computer facility of CSIR-CMMACS and HPC facility at CSIR Institute of Genomics and Integrative Biology.

Competing Interests

The Author(s) declares(s) that there is no competing interest.

Author Contributions

We confirm that the manuscript is original and has not published before. The study was designed by AB, PC and SR, computational screening was done by AB and NI, experiments were done by AB and PC, data analysis was performed by AB, PC, NI and SR, manuscript was written by AB, PC, NI and SR. The manuscript has been read and approved by all